

Normalized Metal Artifact Reduction (NMAR) in Computed Tomography

Esther Meyer, Frank Bergner, Rainer Raupach, Thomas Flohr, and Marc Kachelrieß, *Member, IEEE*

Abstract— Severe artifacts degrade the image quality and the diagnostic value of CT images if metal objects are present in the field of measurement. The standard method for metal artifact reduction (MAR) replaces affected projection data by interpolated data. Often, linear interpolation is used. However, sinogram interpolation introduces new artifacts and lacks accuracy close to metal objects even if more complex interpolation schemes are used. Recently, a method was presented, which uses a simple length normalization of the sinogram prior to interpolation in order to better preserve the contrast between air and water-equivalent objects [1]. However, contrast between objects from different materials, water and bone, for example, is still impaired. We introduce a generalized normalization technique, which concisely preserves details of different materials. This normalization is performed based on a forward projection of a ternary image, which is obtained from a multi-threshold segmentation of the initial image. Simulations and measurements are performed to evaluate our normalized metal artifact reduction method (NMAR) in comparison to standard MAR with linear interpolation and MAR based on simple length normalization. We find considerable improvements in particular for bone structures with metal implants. The improvements are quantified by comparing profiles through images and sinograms for the different methods using simulated data. NMAR clearly outperforms both other methods. We also obtain promising results by applying NMAR to clinical data. This is demonstrated with a scan of a patient with two hip endoprostheses. NMAR is computationally inexpensive, as only parts of a forward projection need to be computed additional to the steps of an interpolation-based MAR. Therefore, our normalization technique can be used as an additional step in any conventional sinogram interpolation-based MAR method.

I. INTRODUCTION

VARIOUS types of metal artifact reduction (MAR) methods have been proposed since the first publications about MAR [2], [3]. Besides interpolation-based approaches, there are statistical- and filtering methods [4], [5], [6]. Other publications which use forward projections to complete missing projection data are references [7], [8]. As shown in reference [9], different methods can be combined successfully. Other interesting approaches which have been pursued include wavelet-filtering and MAR with total variation minimization [10], [11]. Sinogram-based interpolation methods are most widely-spread [3], [12], [13]. The underlying idea of this approach is to consider sinogram values as unreliable if the corresponding rays have intersected metal objects. These values are therefore replaced

by surrogate data, which can be found by linear interpolation, for example, as proposed in reference [3] (we refer to it as MAR1). Metal is found by a thresholding operation in the uncorrected image. Because the CT values of metal are much higher than those of tissue, this is in general an unproblematic step. The metal-only image is subject to a forward projection. Thresholding in the obtained sinogram determines the metal trace, which defines the part of the original rawdata which has to be replaced. After interpolation, the image is reconstructed. A major drawback of pure interpolation methods is the loss of edge information in the metal trace, which results in a blurring of the corresponding edges in the image. Another effect is the introduction of streak artifacts [1]. For reconstruction with filtered backprojection the sinogram is high-pass filtered, which also emphasizes the edge between original and interpolated data. This effect is most pronounced in regions close to metal objects, because a greater part of surrogate sinogram values contributes here. The severely reduced image quality close to implants is especially disturbing, because problems in these regions are often the reason for scanning a patient. It is therefore necessary to pay attention to the proximity of metal objects and avoid the creation of new artifacts there. In reference [1] a length normalization of the sinogram prior to interpolation is used to obtain better contrast between air and water-equivalent objects (MAR2). However, transitions from water to bone are still impaired. We introduce a generalized normalization technique (NMAR), which concisely preserves different materials.

II. METHOD

A. Segmentation

Replacing values in the sinogram by interpolation cannot compensate the lack of information completely. It is therefore desirable to preserve edge information which can already be segmented roughly from the uncorrected image f^{ini} . In reference [1], a binary image f^{bin} is used to separate air and tissue. The binary image is found by thresholding. However, metal implants are often at least partly surrounded by bone. In order to obtain good results in the proximity of the implant, too, a more complex prior image than a binary image has to be used, as this image is used to recover the structure of the projection values which are inpainted in the sinogram. NMAR uses a ternary image f^{tern} in our example. It is obtained by segmentation with two thresholds: t_1 to separate between air and water and t_2 between water and bone. A generalization to a n -ary ver-

Esther Meyer, Frank Bergner and Prof. Dr. Marc Kachelrieß: Institute of Medical Physics (IMP), University of Erlangen–Nürnberg, Henkestr. 91, 91052 Erlangen, Germany.

Dr. Rainer Raupach, Dr. Thomas Flohr: Siemens Healthcare, Siemensstr. 1, 91301 Forchheim, Germany.

Corresponding author: esther.meyer@imp.uni-erlangen.de

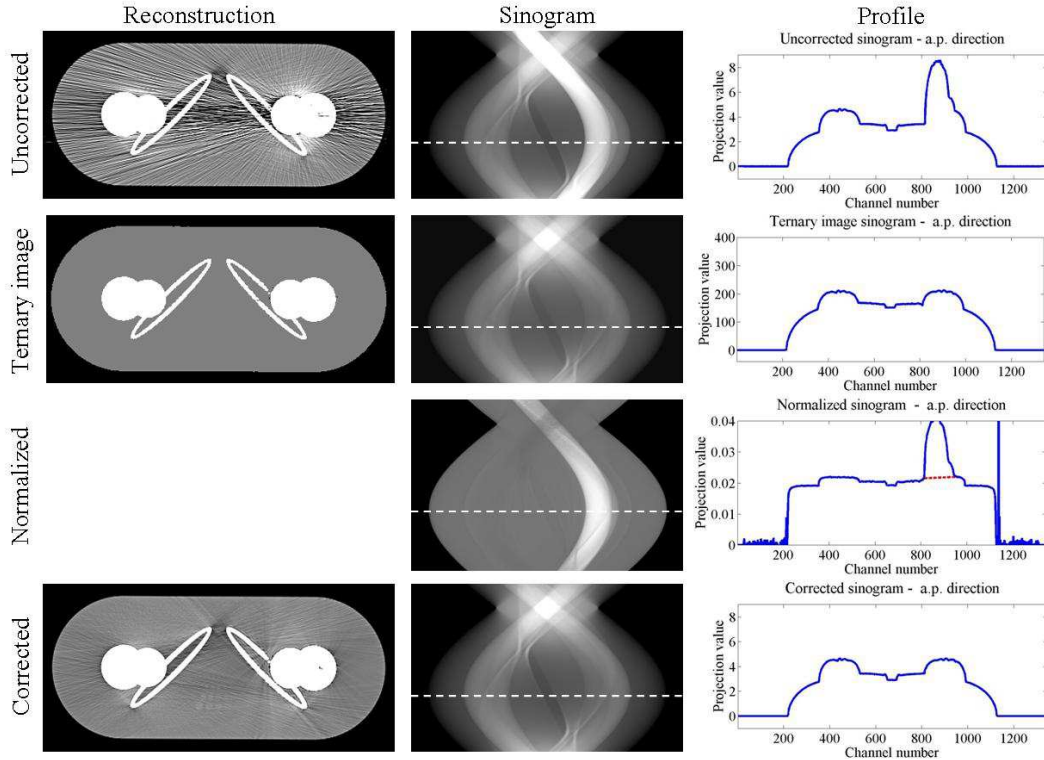


Fig. 1. Steps of NMAR – the images ($C = 0$ HU / $W = 1000$ HU), the corresponding sinograms and a profile through the sinograms are shown. The original data are shown in the top row. The second row contains the ternary image and its sinogram. The sinogram of the ternary image is used for de- and normalization of the original sinogram. The normalized sinogram and a profile through it are displayed in the third row. The dashed line in the profile indicates the interpolated values. The bottom row shows the corrected data.

sion of the method is straightforward. Prior knowledge, for example of the tissue which surrounds the implants, can be used, too. Neighboring slices can be also used to get a more reliable result. In the presence of severe artifacts, using many thresholds most likely leads to artifacts appearing in the segmentation image and thus impairing normalization. Three thresholds lead to good results in our examples. Let μ_{bone} be an average attenuation value for bone. Then the ternary image is defined as:

$$f_{ij}^{\text{tern}} := \begin{cases} 0 & \text{if } f_{ij}^{\text{ini}} < t_1 \\ \mu_{\text{water}} & \text{else if } f_{ij}^{\text{ini}} < t_2 \\ \mu_{\text{bone}} & \text{else.} \end{cases}$$

B. Normalization

Interpolation is less problematic in homogeneous data. The idea of a proper normalization is to transform the sinogram in a way that it becomes comparatively flat. Projection values $p = Rf$ (with Rf being the Radon transform of the scanned object f) depend on the attenuation coefficient of a material, but also on the path length which rays travel through material. The sinogram of an object, consisting of only one material, would attain an average attenuation value everywhere, if each projection value was divided by the corresponding length Rf^{bin} . To generalize this idea to three materials, we divide projections by the forward projected ternary image (for $p^{\text{tern}} > \epsilon > 0$). A small value $\epsilon > 0$ has to be chosen in order to not divide by zero.

This can be understood as interpreting a distance trough a dense material as a longer distance. The normalized projections p^{norm} are subject to an interpolation-based MAR operation M (MAR1 in our experiments). Subsequently, the corrected sinogram p^{corr} is obtained by denormalization of the interpolated, normalized one by multiplying with the projection values p^{tern} :

$$p^{\text{corr}} = p^{\text{tern}} M p^{\text{norm}} = Rf^{\text{tern}} M \frac{p}{Rf^{\text{tern}}}$$

If the initial ternary image is inaccurate, it can be improved by smoothing of f^{ini} and morphological operations. To reduce the streak artifacts prior to the segmentation, smoothing the metal trace as described in reference [1] is beneficial. Figure 1 gives an overview of the different steps of NMAR. The images, the corresponding sinograms and a profile through the sinograms are shown. The original data are displayed in the top row. The second row contains the ternary image and its sinogram. The sinogram of the ternary image contains the important edge information and is used for de- and normalization of the original sinogram. The normalized sinogram and a profile through it are displayed in the third row of the figure. Except for the metal trace, the sinogram is very flat. The dashed line in the profile indicates the interpolated values. The bottom row shows the corrected data. Additional computational costs for NMAR are marginal: Values close to and inside the metal trace are needed for normalization and denor-

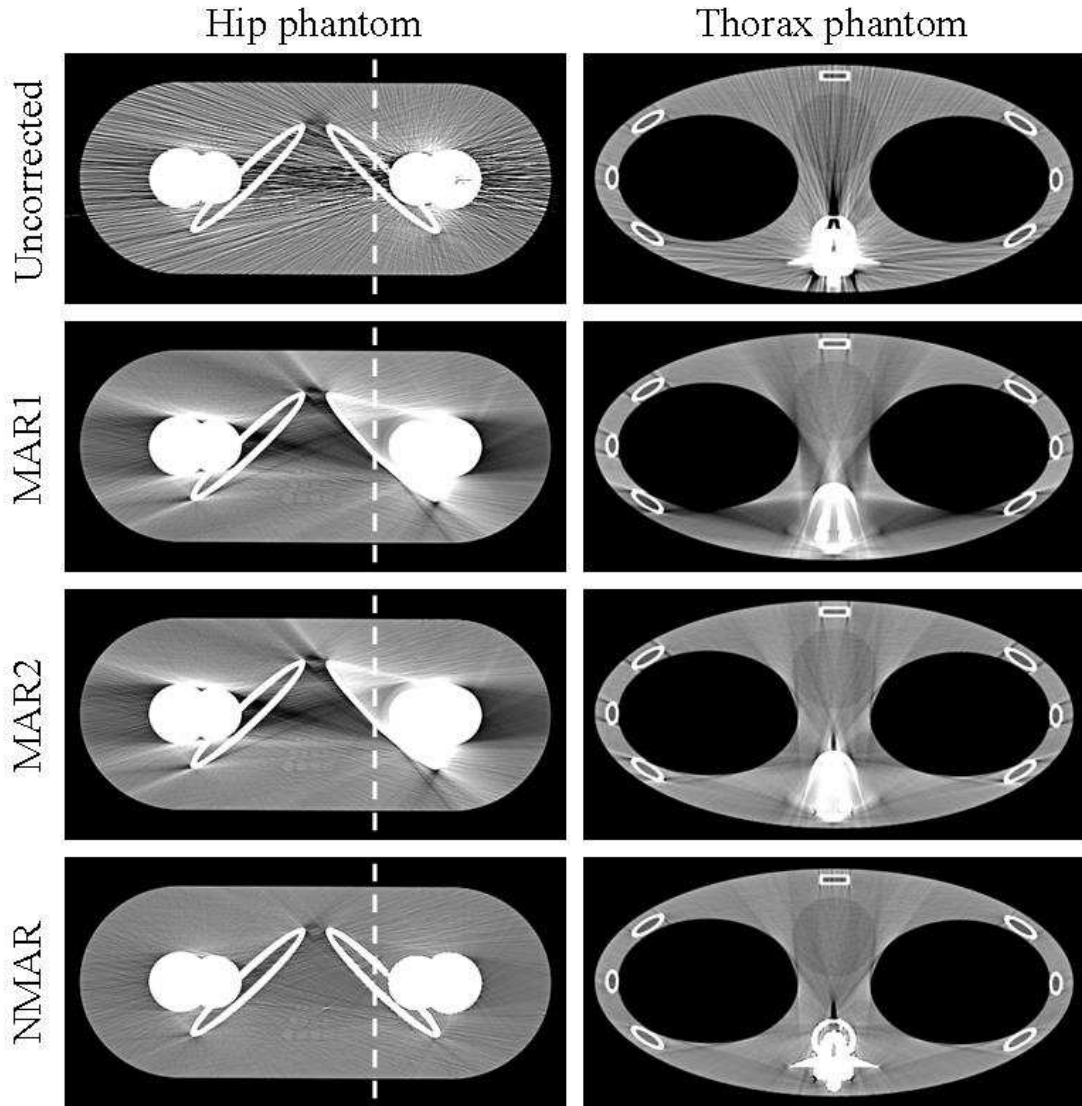


Fig. 2. Method comparison for the simulated hip and thorax phantom – ($C = 0$ HU / $W = 1000$ HU). The streak artifacts are removed successfully by each method. However, MAR1 and MAR2 lead to new artifacts. Images exhibit considerably less artifacts after performing NMAR and the simulations show that even fine bone structures can be preserved. The dashed line indicates the location of the profiles, which are shown in figure 4.

malization, so only small parts of the ternary image have to be forward projected.

III. SIMULATIONS AND MEASUREMENT

We simulate scans of phantoms for two typical clinical situations where metal artifacts occur: Hip replacement by titanium prostheses and spinal fusion using steel screws. Semi-anthropomorphic software phantoms from the FOR-BILD group were simulated, using DRASIM (Siemens Healthcare, Forchheim, Germany). Noise, beam hardening and nonlinear partial volume effects are taken into account. Various different material compositions for soft tissues and bone tissues are simulated. Simulation parameters were 120 kV, 0.6 mm slice width, 672 channels, 1160 views per

rotation. For comparison, we also simulate a noise-free scan of the hip phantom without a metal implant. As we only attempt to reduce metal artifacts, a reconstruction of this scan can serve as a reference image. NMAR was also applied to patient data. The scan of a patient with two hip implants was acquired with a SOMATOM Sensation 16 (140 kV, 320 mAs, 16×0.75 mm collimation, 0.97 spiral pitch) is taken as example. Images are reconstructed with 512×512 pixels, the field of view is 400 mm for the hip phantom and 450 mm for the thorax phantom and for the patient.

IV. RESULTS

The three MAR methods are compared using the two simulations and the patient scan. Reconstructions of the simulated data without correction and corrected by MAR1, MAR2, and NMAR are displayed in figure 2. The streak artifacts are removed successfully by each method. However, MAR1 leads to severe new artifacts in all three cases: blurring of the bone near the implant due to loss of edge information and streak artifacts tangent to the former region of the implant. MAR2 enhances image quality only in case of the thorax phantom, in which the lungs are filled with air. Artifacts close to bones are still present. Images exhibit considerably less artifacts after performing NMAR and the simulations show that even fine bone structures can be preserved.

We analyze the case of the hip phantom more detailed. Figure 3 shows profiles through the different sinograms (original data, reference simulation and after applying MAR1, MAR2 and NMAR). The shape of the projection is preserved only when using NMAR. A profile through the reference image, the uncorrected image and the corrected images are displayed in figure 4. The dashed line in figure 2 indicates the location of the profiles. The profile of the uncorrected image strongly fluctuates due to metal artifacts. In the profiles through images after using MAR1 and MAR2, CT values of bone stay far below the profile through the reference image. Correction with NMAR yields values close to those of the reference profile.

Applying NMAR to clinical data yields promising results, too. For the patient scan, only NMAR results in an image where almost no new streaks are introduced and the bone is clearly visible. The different results are shown in figure 5.

V. CONCLUSION

We introduce and evaluate a generalized sinogram normalization technique, which is designed to prevent the introduction of new artifacts by sinogram interpolation-based MAR methods. The normalization is based on the forward projection of a ternary image, which is obtained by a multi-threshold segmentation. NMAR efficiently reduces metal artifacts in images reconstructed from simulated as well as from clinical data. Image details, especially close to metal objects, are much better preserved compared to MAR using linear interpolation and MAR with a simple length normalization. Our method is computationally inexpensive and can be used as an additional step in any conventional sinogram interpolation-based MAR method.

REFERENCES

- [1] J. Müller and T. M. Buzug, "Spurious structures created by interpolation-based CT metal artifact reduction," *SPIE Medical Imaging Proc.*, vol. 7258, no. 1, pp. 1Y1 – 1Y8, Mar. 2009.
- [2] G. H. Glover and N. J. Pelc, "An algorithm for the reduction of metal clip artifacts in CT reconstructions," *Med. Phys.*, vol. 8, no. 6, pp. 799–807, Nov./Dec. 1981.

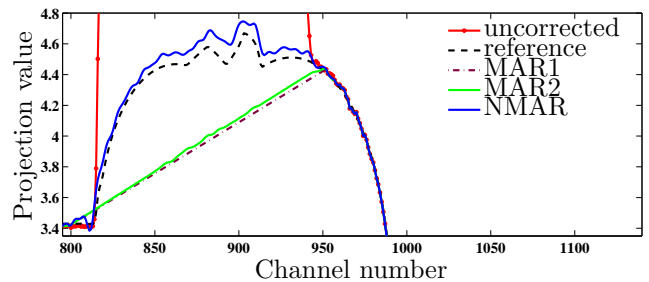


Fig. 3. Sinogram interpolation for the hip phantom – a.p. direction. Shown are profiles through the uncorrected sinogram, the reference simulation and sinograms after correction with MAR1, MAR2 and NMAR. The shape of the projection is preserved only when using NMAR.

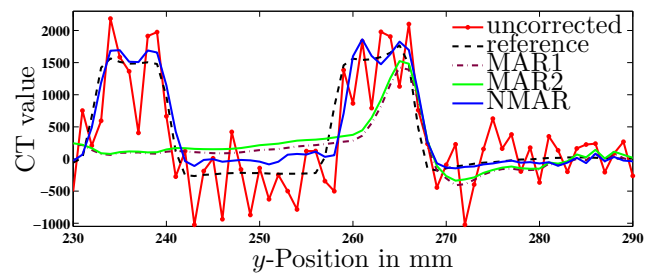


Fig. 4. Profiles through reconstructions of the hip phantom: the initial reconstruction, the reference image and reconstructions after correction with MAR1, MAR2 and NMAR. The profile of the uncorrected image strongly fluctuates due to metal artifacts. In the profiles through images after using MAR1 and MAR2, CT values of bone stay far below the profile through the reference image. Correction with NMAR yields values close to those of the reference profile.

- [3] W. A. Kalender, R. Hebel, and J. Ebersberger, "Reduction of CT artifacts caused by metallic implants," *Radiology*, vol. 164, no. 2, pp. 576–577, Aug. 1987.
- [4] G. Wang, D. L. Snyder, J. A. O'Sullivan, and M. W. Vannier, "Iterative deblurring for CT metal artifact reduction," *IEEE Transactions on Medical Imaging*, vol. 15, no. 5, pp. 657–664, Oct. 1996.
- [5] B. De Man, J. Nuyts, P. Dupont, G. Marchal, and P. Suetens, "An iterative maximum-likelihood polychromatic algorithm for CT," *IEEE Transactions on Medical Imaging*, vol. 20, no. 10, pp. 999–1008, Oct. 2001.
- [6] M. Kachelrieß, O. Watzke, and W. A. Kalender, "Generalized multi-dimensional adaptive filtering (MAF) for conventional and spiral single-slice, multi-slice and cone-beam CT," *Med. Phys.*, vol. 28, no. 4, pp. 475–490, Apr. 2001.
- [7] K. Y. Jeong and J. B. Ra, "Reduction of artifacts due to multiple metallic objects in computed tomography," vol. 7258, no. 1, Jun. 2009, p. 72583E.
- [8] M. Bal and L. Spies, "Metal artifact reduction in ct using tissue-class modeling and adaptive prefiltering," *Medical Physics*, vol. 33, no. 8, pp. 2852–2859, 2006.
- [9] O. Watzke, M. Kachelrieß, and W. A. Kalender, "A pragmatic approach to metal artifact correction in medical CT," *Radiology*, vol. 221(P), pp. 544–545, Nov. 2001.
- [10] S. Zhao, D. D. Robertson, G. Wang, B. Whiting, and K. T. Bae, "X-ray CT metal artifact reduction using wavelets: An application for imaging total hip prostheses," *IEEE Transactions on Medical Imaging*, vol. 19, no. 12, pp. 1238–1247, Dec. 2000.
- [11] X. Duan, L. Zhang, Y. Xiao, J. Cheng, Z. Chen, and Y. Xing, "Metal artifact reduction in CT images by sinogram tv inpainting," in *Nuclear Science Symposium Conference Record, 2008. NSS '08. IEEE*, Oct. 2008, pp. 4175–4177.
- [12] A. H. Mahnken, R. Raupach, J. E. Wildberger, B. Jung, N. Heussen, T. G. Flohr, R. W. Günther, and S. Schaller, "A new algorithm for metal artifact reduction in computed tomogra-

Patient with hip implants

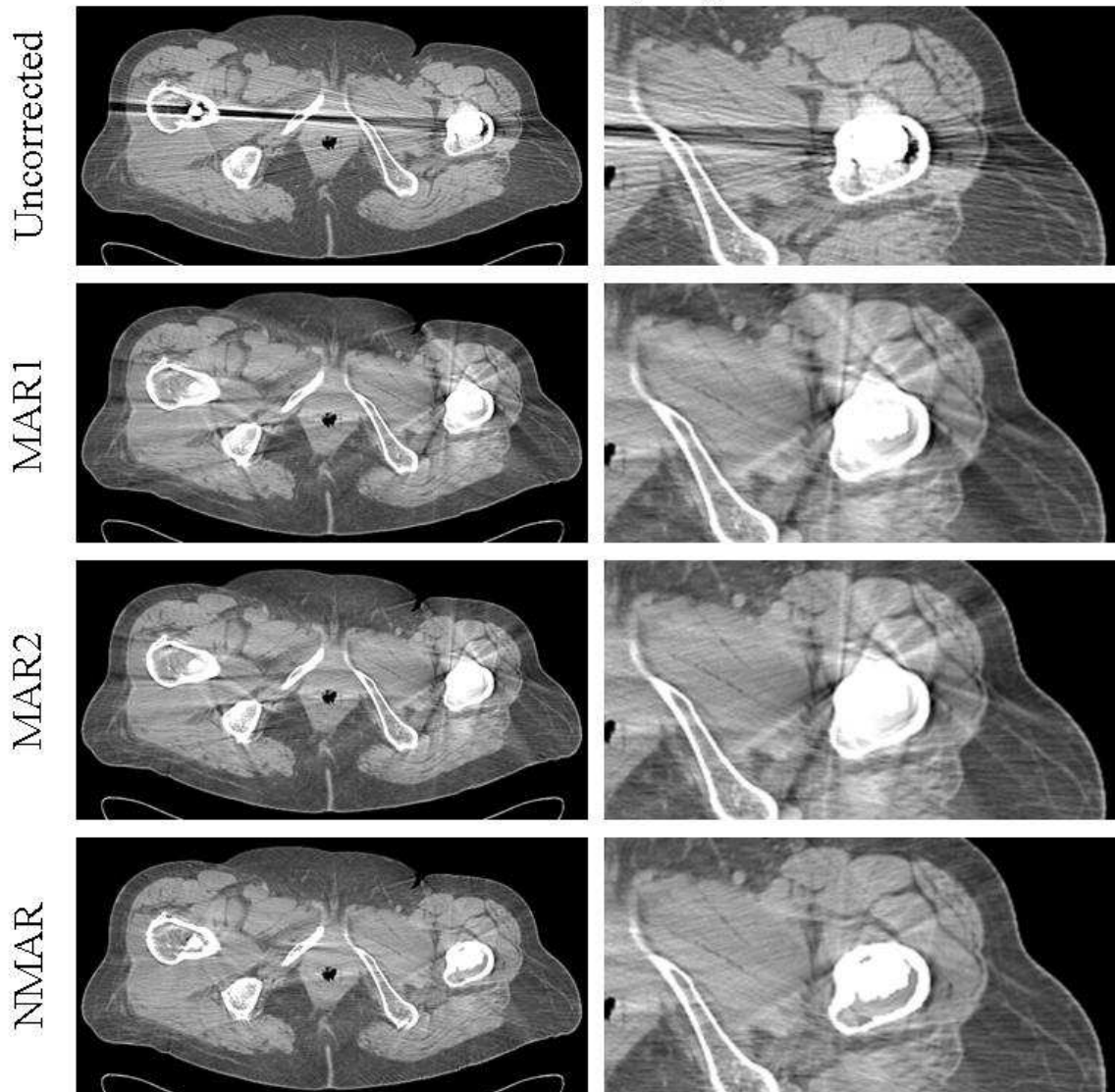


Fig. 5. Method comparison for the scan of a patient with two hip endoprotheses - ($C = 0$ HU / $W = 500$ HU). Only applying NMAR results in an image where almost no new streaks are introduced and the bone near the implant on the right hand side is clearly visible.

- phy: in vitro and in vivo evaluation after total hip replacement,” *Investigative Radiology*, vol. 38, no. 12, pp. 769–775, Dec. 2003.
- [13] J. Wei, L. Chen, G. A. Sandison, Y. Liang, and L. X. Xu, “X-ray CT high-density artefact suppression in the presence of bones,” *Phys. Med. Biol.*, vol. 49, no. 24, pp. 5407–5418, 2004.